

## High-pressure Raman study of $\text{CaV}_2\text{O}_5$

This article has been downloaded from IOPscience. Please scroll down to see the full text article.

2002 J. Phys.: Condens. Matter 14 L583

(<http://iopscience.iop.org/0953-8984/14/32/101>)

View [the table of contents for this issue](#), or go to the [journal homepage](#) for more

Download details:

IP Address: 171.66.16.96

The article was downloaded on 18/05/2010 at 12:20

Please note that [terms and conditions apply](#).

## LETTER TO THE EDITOR

**High-pressure Raman study of  $\text{CaV}_2\text{O}_5$** **Z V Popović<sup>1,4</sup>, V Stergiou<sup>2</sup>, Y S Raptis<sup>2</sup>, M J Konstantinović<sup>1</sup>, M Isobe<sup>3</sup>,  
Y Ueda<sup>3</sup> and V V Moshchalkov<sup>1</sup>**<sup>1</sup> Laboratorium voor Vaste-Stoffysica en Magnetisme, Katholieke Universiteit Leuven,  
Celestijnenlaan 200D, B-3001 Leuven, Belgium<sup>2</sup> Physics Department, National Technical University of Athens, GR 157 80 Athens, Greece<sup>3</sup> Institute for Solid State Physics, The University of Tokyo, 5-1-5 Kashiwanoha, Kashiwa,  
Chiba 277-8581, Japan

Received 7 July 2002

Published 2 August 2002

Online at [stacks.iop.org/JPhysCM/14/L583](http://stacks.iop.org/JPhysCM/14/L583)**Abstract**

The phonon dynamics of the spin ladder calcium vanadium oxide is studied using Raman spectroscopy under high pressure up to 13.5 GPa. Twelve Raman modes, which are observed and assigned at low pressures, disappear at around 9 GPa. With further pressure increase, three broad modes appear at about 325, 750 and 810  $\text{cm}^{-1}$ , indicating the transition of the layered structure into the disordered phase. No scattering activity is found above 13 GPa. The comparison between the vibrational properties of  $\text{CaV}_2\text{O}_5$ ,  $\alpha'$ - $\text{NaV}_2\text{O}_5$  and  $\text{V}_2\text{O}_5$  indicates that anomalous 448  $\text{cm}^{-1}$  mode hardening in  $\alpha'$ - $\text{NaV}_2\text{O}_5$  under pressure is also due to structural changes. The intercalation of Ca atoms results in a higher compressibility and stability of the  $\text{CaV}_2\text{O}_5$  crystal structure in comparison with  $\text{V}_2\text{O}_5$ .

The vanadate oxides,  $\text{AV}_2\text{O}_5$  ( $A = \text{Li}, \text{Na}, \text{Cs}, \text{Mg}$  and  $\text{Ca}$ ), have demonstrated a variety of the low-dimensional quantum spin phenomena, such as one-dimensional antiferromagnetism in  $\alpha'$ - $\text{NaV}_2\text{O}_5$  [1] and  $\text{LiV}_2\text{O}_5$  [2], the antiferromagnetic two-leg ladder structure in  $\text{CaV}_2\text{O}_5$  [3] and  $\text{MgV}_2\text{O}_5$  [2], and the spin-dimer structure in  $\text{CsV}_2\text{O}_5$  [4]. Among all vanadates,  $\alpha'$ - $\text{NaV}_2\text{O}_5$  has attracted much attention in recent years because of the spin-Peierls-like behaviour of its magnetic susceptibility below the transition temperature of 35 K [1]. It has been found that the phase transition is accompanied both by the lattice distortions and a charge ordering.

The calcium vanadate is isostructural with  $\alpha'$ - $\text{NaV}_2\text{O}_5$ . It has an orthorhombic structure [5] with centrosymmetric space group  $Pmnm$  and two formula units per unit cell ( $Z = 2$ ). Each V atom is surrounded by five oxygen atoms, forming  $\text{VO}_5$  pyramids. These pyramids are mutually connected via common edges to form layers in the  $(ab)$ -plane. The Ca atoms are situated between these layers as intercalants. Despite having the same crystal structures, the electronic properties of  $\text{CaV}_2\text{O}_5$  and  $\alpha'$ - $\text{NaV}_2\text{O}_5$  are quite different. In  $\text{CaV}_2\text{O}_5$ , all vanadium

<sup>4</sup> Permanent address: Institute of Physics-Belgrade, PO Box 68, 11080 Belgrade/Zemun, Yugoslavia.

ions are in the  $V^{4+}$  oxidation state and have  $S = 1/2$ .  $\alpha'$ - $NaV_2O_5$  is a mixed-valence compound ( $V^{4+}:V^{5+} = 1:1$ ) with valence electrons attached to the V–O–V molecular orbital of the ladder rung.

The effect of pressure on the structural, vibrational and electronic properties of  $\alpha'$ - $NaV_2O_5$  has been discussed in [6–11]. It has been found that the  $448\text{ cm}^{-1}$  Raman active mode is particularly sensitive to the structural changes induced by pressure. This mode strongly couples with the electronic continuum and corresponds to the bond bending V–O<sub>3</sub>–V vibration. Another important effect is the softening of the V–O<sub>1</sub> Raman active stretching mode under pressure, which appears due to the increased influence of the inter-layer coupling. This observation is not in accordance with x-ray data, which show a shortening of the V–O<sub>1</sub> distance under pressure [7]. Thus, a study of the phonon dynamics in isostructural  $CaV_2O_5$  under pressure, where coupling between phonons and the electronic background is not present, can provide further insight and additional information for the understanding of lattice dynamics in  $\alpha'$ - $NaV_2O_5$  under pressure.

In this letter, we present Raman spectra of  $CaV_2O_5$  polycrystalline samples under pressure. We have found that all Raman lines observed at low pressures disappear at about 9 GPa. Further pressure increase induces three broad bands at about  $325$ ,  $750$  and  $810\text{ cm}^{-1}$ , which clearly indicate a phase transition. No scattering activity is found above 13 GPa. We also discuss the pressure dependences of the highest frequency modes of  $CaV_2O_5$  through comparison with the corresponding modes in  $\alpha'$ - $NaV_2O_5$  and  $V_2O_5$ .

High-pressure Raman scattering measurements were carried out at room temperature, using a gasketed diamond anvil cell (DAC) [12]. The powder samples were loaded into the cell, with a 4:1 methanol/ethanol mixture as a pressure medium. The details of the sample preparation have been published elsewhere [3]. The standard ruby luminescence was used for pressure calibration. Ar-ion lasers were used as the excitation source. The scattered light was dispersed with a Spex 1403 double monochromator and detected with a conventional photon counting system.

The unpolarized Raman spectra of  $CaV_2O_5$  at ambient ( $p = 0.1\text{ MPa}$ ) and high pressures are presented in figure 1. The effect of pressure on the mode frequencies is illustrated in figure 2. The lines show a polynomial ( $\omega = A + B_1 p + B_2 p^2$ ) fit. The best fit parameters are given in table 1. By comparing the ratio of  $B_2$  over  $B_1$  for different modes, we observe (see table 1) that for the highest frequency mode at  $932\text{ cm}^{-1}$ , as well as for the  $470\text{ cm}^{-1}$  mode, this ratio takes a significantly higher value than the corresponding ratio of all other modes having this ratio as a negative value. The frequencies of all other modes move to higher energies with pressure, without any peculiarity such as crossing, anti-crossing, overlapping or intensity exchange. This result suggests that almost all lattice parameters decrease with increasing pressure while maintaining the same inter-layer and intra-layer symmetry.

The assignment of the observed Raman active modes given in figure 2 is done by comparing mode intensities for parallel and crossed polarized configurations [13, 14] with fully polarized spectra of  $\alpha'$ - $NaV_2O_5$  [15]. Despite the same crystal structure of  $CaV_2O_5$  and  $\alpha'$ - $NaV_2O_5$  there is a remarkable difference in frequencies for some analogous phonon modes, mostly due to the difference in interatomic distances, and the electronic structure. The highest frequency  $A_{1g}$  phonon mode appears at  $932\text{ cm}^{-1}$  in  $CaV_2O_5$  Raman spectra. This mode represents the V–O<sub>1</sub> bond stretching vibration, see inset in figure 3(a). The larger V–O<sub>1</sub> distance in  $CaV_2O_5$  ( $1.645\text{ \AA}$ , [5]), in comparison with the corresponding interatomic distance in  $\alpha'$ - $NaV_2O_5$  ( $1.61\text{ \AA}$  [16]), causes the frequency shift of this phonon to lower energies. The same conclusion can be made for the highest frequency  $CaV_2O_5$  mode with  $B_{1g}$  symmetry at  $636\text{ cm}^{-1}$ . This mode originates from the bond stretching vibrations of the V and the O<sub>2</sub> ions along the *b*-axis, see inset in figure 3(d). The next  $A_{1g}$  mode of  $CaV_2O_5$  appears at the frequency of  $539\text{ cm}^{-1}$  which is close to the frequency of the analogous mode in  $\alpha'$ - $NaV_2O_5$  ( $534\text{ cm}^{-1}$ ).

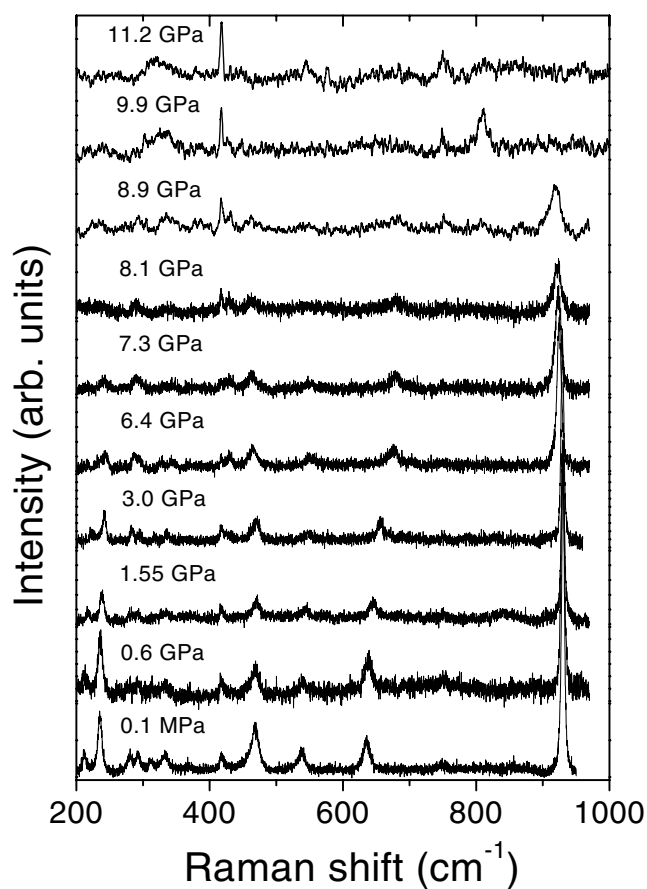


**Figure 1.** Unpolarized Raman spectra of  $\text{CaV}_2\text{O}_5$  at room temperature and different pressures.

**Table 1.** Frequencies and pressure coefficients of Raman active modes of  $\text{CaV}_2\text{O}_5$ .  $\omega$  represents the mode frequencies at ambient conditions.  $B_1$ ,  $B_2$  and  $A$  are the linear, quadratic and free terms of the polynomial fit  $\omega = A + B_1 p + B_2 p^2$ , respectively.

$\omega$ ( $\text{cm}^{-1}$ )	$A$ ( $\text{cm}^{-1}$ )	$B_1$ ( $\text{cm}^{-1} \text{ GPa}^{-1}$ )	$B_1/A$ ( $10^{-2} \text{ GPa}^{-1}$ )	$B_2$ ( $\text{cm}^{-1} \text{ GPa}^{-2}$ )	$B_2/B_1$ ( $1 \text{ GPa}^{-1}$ )
90	90.3	0.18	0.2	0.214	1.19
212	211	5.48	2.6	-0.284	-0.052
236	235	3.0	1.28	-0.265	-0.088
281	280	0.63	0.22	0.0725	0.115
293	291	1.77	0.61	-0.142	-0.080
310	311	1.946	0.626	0.001	0.051
335	332	1.94	0.584	-0.0614	-0.031
418	417.5	0.59	0.14	0.0967	0.16
470	468	0.856	0.183	-0.181	-0.21
539	537	4.465	0.83	-0.37	-0.083
636	634	9.02	1.425	-0.386	-0.043
932	931	0.165	0.018	-0.147	-0.89

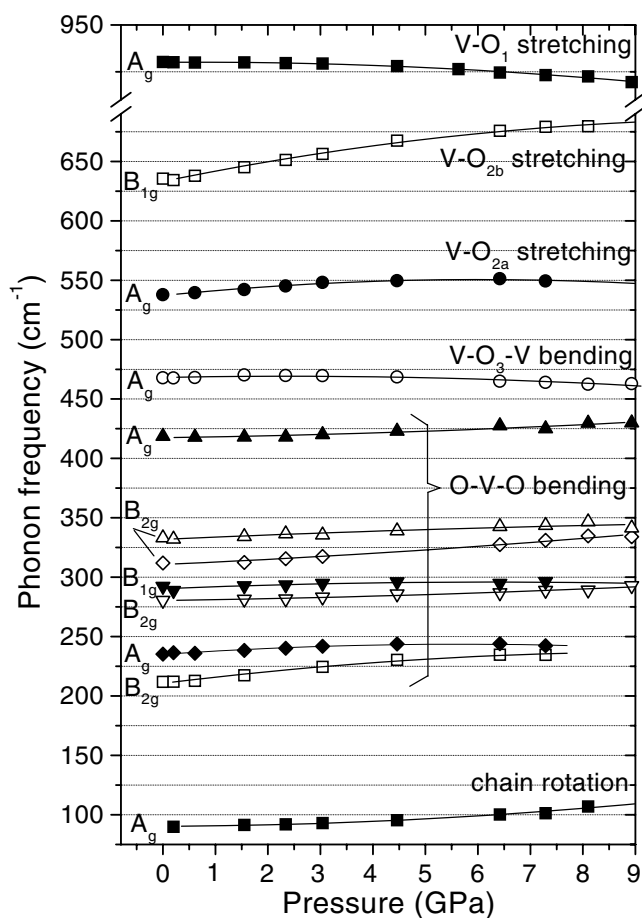


**Figure 2.** Pressure dependence of Raman mode frequencies of  $\text{CaV}_2\text{O}_5$ . The solid curves are polynomial fits obtained with parameters given in table 1.

This mode represents the bond stretching vibration of V and  $\text{O}_{2a}$  ions, see inset in figure 3(b). The lack of any noticeable frequency difference between these modes is in accordance with a similar value of the V– $\text{O}_{2a}$  bond length in  $\text{CaV}_2\text{O}_5$  (1.982 Å) and  $\alpha'$ - $\text{NaV}_2\text{O}_5$  (1.985 Å).

According to the crystallographic data, the V– $\text{O}_3$ –V bond bending mode of  $\text{CaV}_2\text{O}_5$  at  $470\text{ cm}^{-1}$  (mainly  $\text{O}_3$  ion vibrations along the  $c$ -axis, see inset in figure 3(c)) should appear at a frequency lower than the frequency of the analogous mode in  $\alpha'$ - $\text{NaV}_2\text{O}_5$  ( $448\text{ cm}^{-1}$ ), because the V– $\text{O}_3$ –V bond length in  $\text{CaV}_2\text{O}_5$  (3.81 Å) is larger than that of  $\alpha'$ - $\text{NaV}_2\text{O}_5$  (3.64 Å). This apparent discrepancy is easy to understand if we bear in mind that the renormalized frequency (no electron–phonon interaction) of the V– $\text{O}_3$ –V bond bending mode in  $\alpha'$ - $\text{NaV}_2\text{O}_5$  ( $\text{V}_2\text{O}_5$ ) is at  $485\text{ cm}^{-1}$  [15] ( $483\text{ cm}^{-1}$  [17]).

In figure 3 we compare the pressure-induced frequency shifts of the four highest frequency modes in  $\text{CaV}_2\text{O}_5$ ,  $\alpha'$ - $\text{NaV}_2\text{O}_5$  and  $\text{V}_2\text{O}_5$ . Besides similarities in the crystal structure (all of them have the same layered structure built from the edge sharing  $\text{VO}_5$  square pyramids) these compounds differ with respect to the formal oxidation state of the V ions, which is 4+ in  $\text{CaV}_2\text{O}_5$ , 4.5+ in  $\alpha'$ - $\text{NaV}_2\text{O}_5$  and 5+ in  $\text{V}_2\text{O}_5$ . As can be seen in figure 3, the highest frequency modes of the  $\text{A}_{1g}$  (figure 3(a)) and the  $\text{B}_{1g}$  (figure 3(d)) symmetries have the same kind of mode

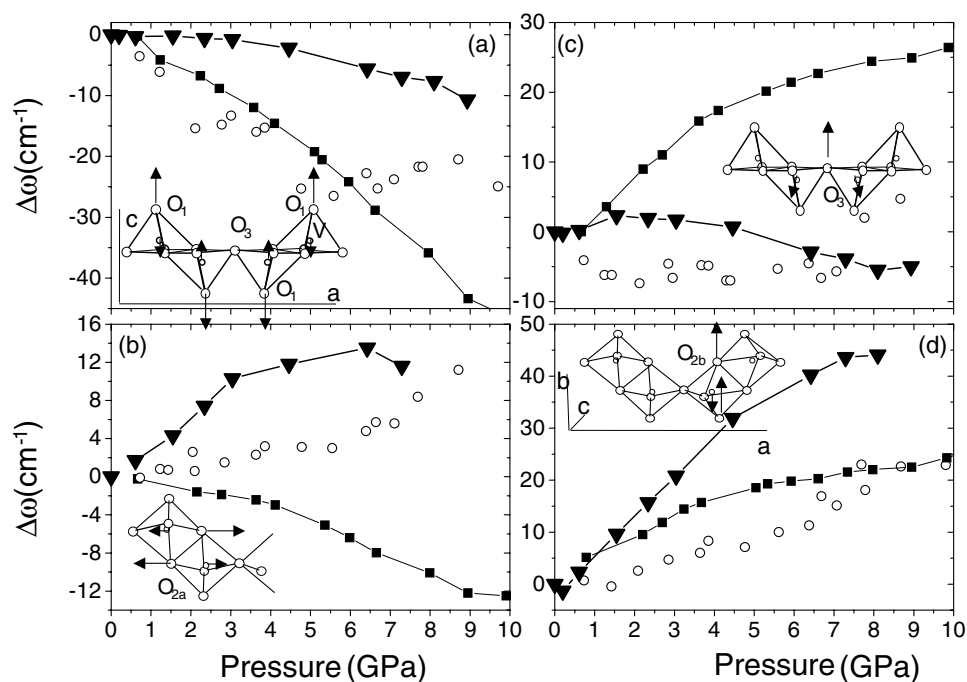


**Figure 3.** Pressure frequency shift of several Raman modes of  $\text{CaV}_2\text{O}_5$  (▼) in comparison with the corresponding modes of  $\alpha'$ - $\text{NaV}_2\text{O}_5$  (■) and  $\text{V}_2\text{O}_5$  (○). The insets show the ion displacement patterns of the corresponding modes: (a) the V– $\text{O}_1$  bond stretching  $A_{1g}$  symmetry mode at  $969\text{ cm}^{-1}$  ( $\alpha'$ - $\text{NaV}_2\text{O}_5$ ),  $932\text{ cm}^{-1}$  ( $\text{CaV}_2\text{O}_5$ ),  $997\text{ cm}^{-1}$  ( $\text{V}_2\text{O}_5$ ); (b) the V– $\text{O}_{2a}$  bond stretching  $A_{1g}$  symmetry mode at  $534\text{ cm}^{-1}$  ( $\alpha'$ - $\text{NaV}_2\text{O}_5$ ),  $539\text{ cm}^{-1}$  ( $\text{CaV}_2\text{O}_5$ ),  $524\text{ cm}^{-1}$  ( $\text{V}_2\text{O}_5$ ); (c) the V– $\text{O}_3$ –V bond bending  $A_{1g}$  symmetry mode at  $448\text{ cm}^{-1}$  ( $\alpha'$ - $\text{NaV}_2\text{O}_5$ ),  $470\text{ cm}^{-1}$  ( $\text{CaV}_2\text{O}_5$ ),  $478\text{ cm}^{-1}$  ( $\text{V}_2\text{O}_5$ ); (d) the V– $\text{O}_{2b}$  bond stretching  $B_{1g}$  symmetry mode at  $684\text{ cm}^{-1}$  ( $\alpha'$ - $\text{NaV}_2\text{O}_5$ ),  $636\text{ cm}^{-1}$  ( $\text{CaV}_2\text{O}_5$ ), and  $702\text{ cm}^{-1}$  ( $\text{V}_2\text{O}_5$ ).

frequency versus pressure dependence in all three compounds. The  $A_{1g}$  modes at  $539\text{ cm}^{-1}$  (figure 3(b)) and  $470\text{ cm}^{-1}$  (figure 3(c)) have opposite frequency versus pressure dependence in  $\alpha'$ - $\text{NaV}_2\text{O}_5$  and in  $\text{CaV}_2\text{O}_5$  ( $\text{V}_2\text{O}_5$ ).

The V– $\text{O}_1$  bond stretching mode (see figure 3(a)) softens with increasing pressure in all three compounds. The softening is much stronger in  $\alpha'$ - $\text{NaV}_2\text{O}_5$  ( $50\text{ cm}^{-1}$  at  $p = 10\text{ GPa}$ ) and  $\text{V}_2\text{O}_5$  ( $25\text{ cm}^{-1}$  at  $p = 6\text{ GPa}$  [18]) than in  $\text{CaV}_2\text{O}_5$  ( $11\text{ cm}^{-1}$  at  $p = 9\text{ GPa}$ ). The strong softening of the V– $\text{O}_1$  stretching mode in  $\alpha'$ - $\text{NaV}_2\text{O}_5$  and  $\text{V}_2\text{O}_5$  is due to the increase influence of the inter-layer  $\text{V}\cdots\text{O}_1$  bond under pressure, which leads to a continuous change in the V coordination from square pyramidal towards octahedral [9, 10, 18]. In the case of  $\text{CaV}_2\text{O}_5$ , due to the larger Ca ion radius, the inter-layer interaction is reduced, and softening is considerably smaller.

The pressure-induced frequency shift of the V– $\text{O}_{2a}$  bond stretching mode at  $539\text{ cm}^{-1}$  in  $\text{CaV}_2\text{O}_5$  is positive (see figure 3(b)) and somewhat stronger than in  $\text{V}_2\text{O}_5$ . The negative frequency shift of the corresponding mode in  $\alpha'$ - $\text{NaV}_2\text{O}_5$  is, most probably, a consequence of coupling between this mode and the electronic background peaked at about  $650\text{ cm}^{-1}$ . This type of electronic background is not presented either in  $\text{CaV}_2\text{O}_5$  or in  $\text{V}_2\text{O}_5$ .

The most intriguing pressure dependence is observed for the V– $\text{O}_3$ –V bond bending vibration. This mode hardens by  $25\text{ cm}^{-1}$  in  $\alpha'$ - $\text{NaV}_2\text{O}_5$  when the pressure is increased

to 10 GPa [9]. The corresponding modes in  $\text{CaV}_2\text{O}_5$  and  $\text{V}_2\text{O}_5$  show (figure 3(c)) a very small frequency shift under pressure. Such a large difference between Na and Ca vanadate pressure dependences for this mode can be due to change in the electronic structure, and/or due to the structural changes.

According to the V–O<sub>3</sub>–V bond length in these three compounds (3.81 Å in  $\text{CaV}_2\text{O}_5$ , 3.64 Å in  $\alpha'$ - $\text{NaV}_2\text{O}_5$ , 3.56 Å in  $\text{V}_2\text{O}_5$  [17]), the V–O<sub>3</sub>–V bond bending vibration in  $\alpha'$ - $\text{NaV}_2\text{O}_5$  should have an energy higher than in  $\text{CaV}_2\text{O}_5$  and smaller than in  $\text{V}_2\text{O}_5$ . However, the presence of a single electron in the V–O<sub>3</sub>–V rung of  $\alpha'$ - $\text{NaV}_2\text{O}_5$  strongly affects the bond bending force constant and shifts the energy to 448 cm<sup>-1</sup>. As a consequence, the charge ordering transition ( $T_c = 34$  K) is expected to have fingerprints in the energy versus temperature behaviour of this mode, which is not observed. Such an intriguing dissonance is similar to the observed mode behaviour under pressure, thus indicating that simple structural changes may be behind these findings. Indeed, the V–O<sub>3</sub>–V bond length in  $\alpha'$ - $\text{NaV}_2\text{O}_5$  decreases from 3.64 Å at ambient pressure to 3.56 Å (3.52 Å) at 5.4 GPa (15.5 GPa) [7]. We make an approximate estimation for the change of the bond bending force constant by scaling the frequency as the square root of the force constant, and assuming a scaling of the force constants as  $R^{-6}$  ( $R$  is the bond length). Similarly, scaling of the phonon frequency for the bond stretching mode is  $R^{-3}$ . In our case,  $R(\text{O–V}_3\text{–O})_0/R(\text{O–V}_3\text{–O})_{5.6\text{GPa}}$  is 1.0225. This parameter can produce an increase of the phonon frequency of about 7% (about 30 cm<sup>-1</sup> in the case of  $\omega = 448$  cm<sup>-1</sup>), which is enough to explain the observed phonon frequency shift of the V–O<sub>3</sub>–V bond bending mode under pressure.

Finally, in figure 3(d) we compare the frequency versus pressure dependences of the V–O<sub>2b</sub> bond stretching mode. This mode represents the out-of-phase bond stretching vibration of the B<sub>1g</sub> symmetry. The large frequency shift of this mode under pressure in  $\text{CaV}_2\text{O}_5$  is related to a larger compressibility along the  $b$ -axis in  $\text{CaV}_2\text{O}_5$  (the V–O<sub>2b</sub> distance in  $\text{CaV}_2\text{O}_5$  is about 2% larger than in  $\alpha'$ - $\text{NaV}_2\text{O}_5$ ).

Let us refer back to figure 1. A dramatic spectral change occurs above 9 GPa, where the strongest peak of  $\text{CaV}_2\text{O}_5$  at 932 cm<sup>-1</sup> also disappears. At the same pressure (10 GPa) three broad modes appear at ~325, 750 and 810 cm<sup>-1</sup>. At a pressure of 11.2 GPa the mode at about 750 cm<sup>-1</sup> becomes more intense than the 810 cm<sup>-1</sup> mode and a broad structure at about 650 cm<sup>-1</sup> starts to develop. The shape and frequency of these modes correspond to those of amorphous  $\text{NaVO}_3$  [19]. This means that the pressure of 10 GPa causes complete breakdown of the  $\text{CaV}_2\text{O}_5$  crystal structure, keeping short-range ordering up to 13 GPa.

In conclusion, we have studied the Raman scattering in spin ladder calcium vanadium oxide under high pressure up to 13.5 GPa. Twelve modes, which are observed and assigned at low pressures, disappear at around 9 GPa. With further pressure increase, three broad modes appear at about 325, 750 and 810 cm<sup>-1</sup>, indicating the transition of the layered structure of  $\text{CaV}_2\text{O}_5$  into a disordered phase. No scattering activity is found above 13 GPa. Finally, a comparison between the pressure dependence of four distinctive modes of  $\text{CaV}_2\text{O}_5$ ,  $\alpha'$ - $\text{NaV}_2\text{O}_5$  and  $\text{V}_2\text{O}_5$  is presented in terms of their crystallographic as well as V-oxidation states.

This work was supported by the Serbian Ministry of Science and Technology, by the National Technical University, Athens, and by the GOA and FWO projects at K U Leuven.

## References

- [1] Isobe M and Ueda Y 1996 *J. Phys. Soc. Japan* **65** 1178
- [2] Isobe M, Ueda Y, Takizawa K and Goto T 1998 *J. Phys. Soc. Japan* **67** 755

- [3] Iwase H, Isobe M, Ueda Y and Yasuoka H 1996 *J. Phys. Soc. Japan* **65** 2397
- [4] Isobe M and Ueda Y 1996 *J. Phys. Soc. Japan* **65** 3142
- [5] Onoda M and Nishiguchi N 1996 *J. Solid State Chem.* **127** 359
- [6] Nakao H, Ohwada K, Takesue N, Fujii Y, Isobe M, Ueda Y, Sawa H, Kawada H, Murakami Y, David W I F and Ibberson R M 1998 *Physica B* **241-3** 534
- [7] Loa I, Syassen K, Kremer R K, Schwarz U and Hanfland M 1999 *Phys. Rev. B* **60** R6945
- [8] Loa I, Syassen K and Kremer R K 1999 *Solid State Commun.* **112** 681
- [9] Loa I, Schwarz U, Hanfland M, Kremer R K and Syassen K 1999 *Phys. Status Solidi b* **215** 709
- [10] Loa I, Grzechnik A, Schwarz U, Syassen K, Hanfland M and Kremer R K 2001 *J. Alloys Compounds* **317-18** 103
- [11] Ohwada K, Fujii Y, Takesue N, Isobe M, Ueda Y, Nakao H, Wakabayashi Y, Murakami Y, Ito K, Amemiya Y, Fujihisa H, Aoki K, Noda Y and Ikeda N 2001 *Phys. Rev. Lett.* **87** 086402
- [12] Huber G, Syassen K and Holzapfel W B 1977 *Phys. Rev. B* **15** 5123
- [13] Konstantinović M J, Popović Z V, Isobe M and Ueda Y 2000 *Phys. Rev. B* **61** 15 185
- [14] Popović Z V, Konstantinović M J, Gajić R, Popov V, Isobe M, Ueda Y and Moshchalkov V V 2002 *Phys. Rev. B* **65** 184303
- [15] Popović Z V, Konstantinović M J, Gajić R, Popov V, Raptis Y S, Vasil'ev A N, Isobe M and Ueda Y 1999 *Solid State Commun.* **110** 381
- [16] Onoda M and Nishiguchi N 1999 *J. Phys.: Condens. Matter* **11** 3475
- [17] Clauws P, Broeckx J and Vennik J 1985 *Phys. Status Solidi b* **131** 459
- [18] Grzechnik A 1998 *Chem. Mater.* **10** 2505
- [19] Shen Z X, Ong C W, Tang S H and Kuok M H 1994 *J. Phys. Chem. Solids* **55** 661  
Shen Z X, Ong C W, Tang S H and Kuok M H 1994 *J. Phys. Chem. Solids* **55** 665  
Shen Z X, Ong C W, Tang S H and Kuok M H 1994 *Phys. Rev. B* **49** 1433